

Global Chemical Composition of Ambient Fine Particulate Matter for Exposure Assessment

Sajeev Philip,^{*,†} Randall V. Martin,^{†,‡} Aaron van Donkelaar,[†] Jason Wai-Ho Lo,[†] Yuxuan Wang,[§] Dan Chen,^{||} Lin Zhang,[⊥] Prasad S. Kasibhatla,[#] Siwen Wang,[○] Qiang Zhang,[▽] Zifeng Lu,[◆] David G. Streets,[◆] Shabtai Bittman,[¶] and Douglas J. Macdonald^{††}

[†]Department of Physics and Atmospheric Science, Dalhousie University, Halifax, Nova Scotia B3H 4R2, Canada

[‡]Harvard-Smithsonian Center for Astrophysics, Cambridge, Massachusetts 02138, United States

[§]Ministry of Education Key Laboratory for Earth System Modeling, Center for Earth System Science, Institute for Global Change Studies, [○]State Key Joint Laboratory of Environment Simulation and Pollution Control, School of Environment, and [▽]Center for Earth System Science, Tsinghua University, Beijing 100084, China

^{||}Department of Atmospheric and Oceanic Sciences, University of California, Los Angeles, California 90095, United States

[⊥]Department of Atmospheric and Oceanic Sciences, School of Physics, Peking University, Beijing 100871, China

[#]Nicholas School of the Environment and Earth Sciences, Duke University, Durham, North Carolina 27708, United States

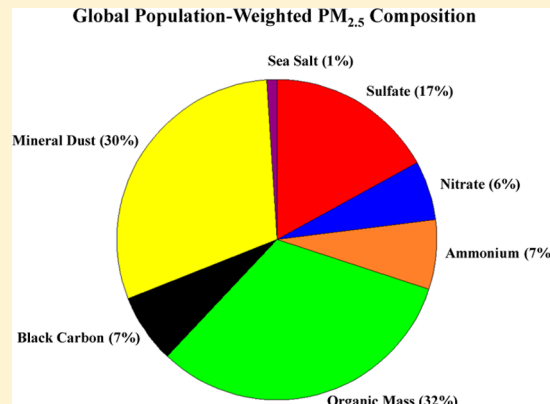
[◆]Decision and Information Sciences Division, Argonne National Laboratory, Argonne, Illinois 60439, United States

[¶]Agriculture and Agri-Food Canada, Agassiz, British Columbia V0M 1A2, Canada

^{††}Environment Canada, Gatineau, Quebec K1A 0H3, Canada

Supporting Information

ABSTRACT: Epidemiologic and health impact studies are inhibited by the paucity of global, long-term measurements of the chemical composition of fine particulate matter. We inferred PM_{2.5} chemical composition at 0.1° × 0.1° spatial resolution for 2004–2008 by combining aerosol optical depth retrieved from the MODIS and MISR satellite instruments, with coincident profile and composition information from the GEOS-Chem global chemical transport model. Evaluation of the satellite-model PM_{2.5} composition data set with North American in situ measurements indicated significant spatial agreement for secondary inorganic aerosol, particulate organic mass, black carbon, mineral dust, and sea salt. We found that global population-weighted PM_{2.5} concentrations were dominated by particulate organic mass (11.9 ± 7.3 μg/m³), secondary inorganic aerosol (11.1 ± 5.0 μg/m³), and mineral dust (11.1 ± 7.9 μg/m³). Secondary inorganic PM_{2.5} concentrations exceeded 30 μg/m³ over East China. Sensitivity simulations suggested that population-weighted ambient PM_{2.5} from biofuel burning (11 μg/m³) could be almost as large as from fossil fuel combustion sources (17 μg/m³). These estimates offer information about global population exposure to the chemical components and sources of PM_{2.5}.



INTRODUCTION

A large body of evidence has established that short-term human exposure to various chemical constituents of particulate matter (PM) with aerodynamic diameter less than 2.5 μm (PM_{2.5}) is associated with adverse health effects including increased hospital admissions (e.g., refs 1–3), cardiovascular, respiratory, and all-cause mortality (e.g., refs 4–8). However, the health impacts of long-term exposure to PM_{2.5} chemical components are less well understood, in contrast to the well-established relationship of the total PM_{2.5} mass with adverse health effects (e.g., refs 9–11). Epidemiologic and health impact assessments of PM_{2.5} composition have been impeded by the paucity of long-

term measurements of PM_{2.5} composition. Spatial mapping of aerosol composition could help in elucidating the health impacts of fine particulate matter components.

Satellite remote sensing for surface air quality has developed rapidly over the past decade.^{12,13} Aerosol optical depth (AOD), an optical measure of the column integrated aerosol abundance in the atmosphere, can now be reliably retrieved from satellite

Received: June 18, 2014

Revised: October 21, 2014

Accepted: October 24, 2014

Published: October 24, 2014

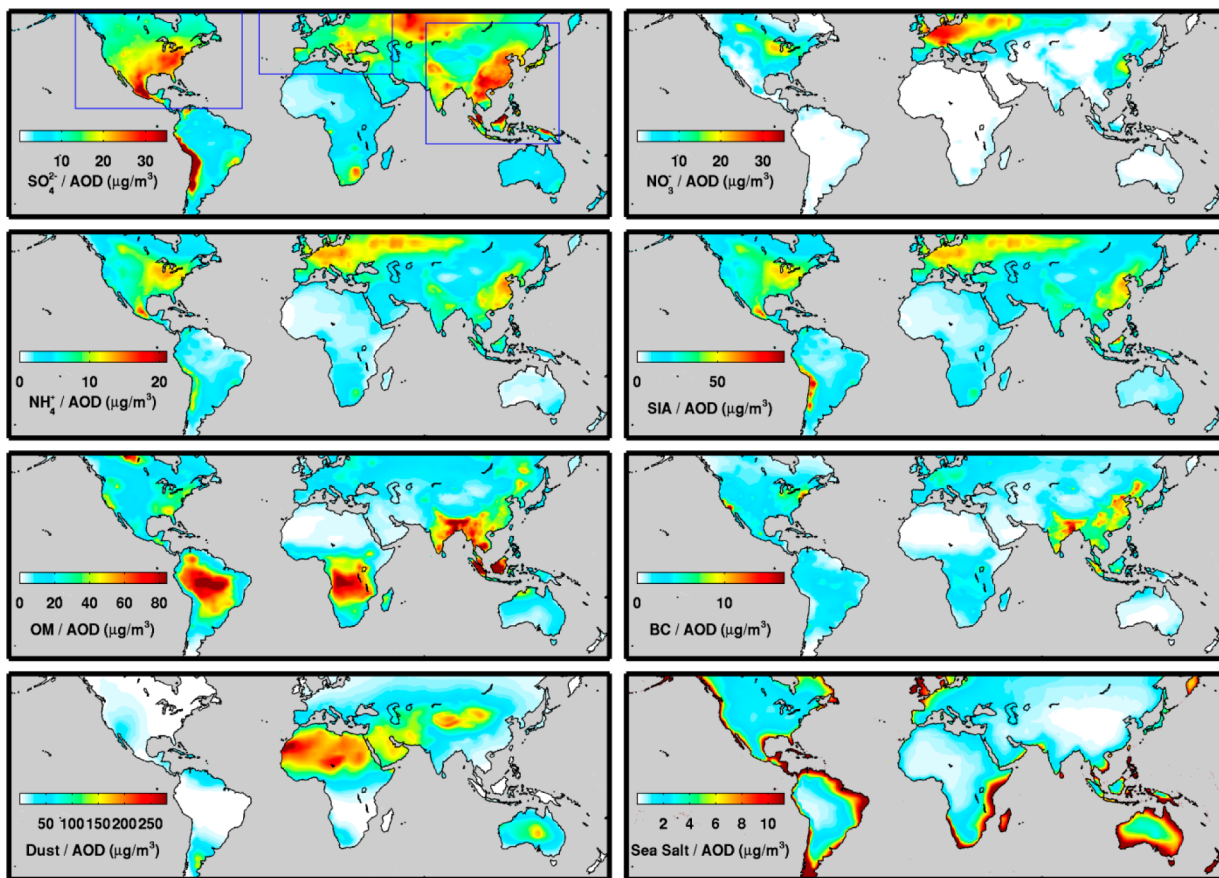


Figure 1. Mean ratio of $\text{PM}_{2.5}$ composition to AOD for 2004–2008. $\text{PM}_{2.5}$ composition is represented as dry mass. Abbreviations are Secondary Inorganic Aerosol (SIA; the sum of SO_4^{2-} , NO_3^- , and NH_4^+), Organic Mass (OM), and Black Carbon (BC). Gray denotes water. The top-left panel contains the boundaries of the three nested GEOS-Chem regions.

remote sensing over land. Several studies have demonstrated close relationships between AOD and $\text{PM}_{2.5}$ (e.g., refs 14–16) to the point that AOD is being used for operational air quality forecasting.^{17,18} However, the relation of AOD with $\text{PM}_{2.5}$ is complex,¹⁹ and, despite progress in retrieving aerosol composition from satellite,^{20,21} current satellite instrumentation provides incomplete information on the chemical composition of $\text{PM}_{2.5}$.¹³

Chemical transport models (CTMs) also have developed markedly over the past decade. Current CTMs are capable of simulating the atmospheric distribution of aerosols and of calculating the local, coincident relationship of satellite AOD with ground-level $\text{PM}_{2.5}$ concentration at a regional²² and global²³ scale. CTMs also offer the capability to simulate the major chemical components of $\text{PM}_{2.5}$ including secondary inorganic aerosol (sulfate, nitrate, and ammonium), primary and secondary organic aerosol, black carbon, mineral dust, sea salt, and aerosol water. These model developments offer information about the relation of AOD with ground-level $\text{PM}_{2.5}$ and its chemical composition. CTMs are also being used to quantify the contributions of specific emission sources to $\text{PM}_{2.5}$ to inform mitigation strategies (e.g., refs 24 and 25).

Scientific understanding of $\text{PM}_{2.5}$ chemical composition has been closely coupled with advances in measurements. For example, several in situ monitoring networks across the U.S. and Canada routinely measure the major components of $\text{PM}_{2.5}$ (e.g., refs 26 and 27). Numerous studies combined these in situ data to study the spatial and temporal variation of $\text{PM}_{2.5}$ chemical composition (e.g., refs 28–30). Other established networks are

the European Monitoring and Evaluation Programme (EMEP; <http://www.emep.int/>) and the Acid Deposition Monitoring Network in East Asia (EANET; <http://www.eanet.cc/>) which measure some components of $\text{PM}_{2.5}$. Research measurements offer additional valuable data. These in situ measurements are too sparse to fully represent population exposure across the world. However, they provide an opportunity to evaluate $\text{PM}_{2.5}$ composition inferred from satellite remote sensing and modeling (hereafter, satellite-model).

We combined satellite-derived AOD with global modeling of coincident aerosol vertical profile and composition to produce a global long-term (2004–2008) mean ambient outdoor satellite-model $\text{PM}_{2.5}$ composition data set at a spatial resolution of $0.1^\circ \times 0.1^\circ$. We evaluated this data set with in situ measurements across North America and where available in the rest of the world. We combined model sensitivity simulations with satellite-derived AOD to estimate three major emission sources of total $\text{PM}_{2.5}$ mass. We subsequently estimated the population-weighted concentrations of ambient $\text{PM}_{2.5}$ chemical components and its major emission sources.

MATERIALS AND METHODS

Processing Satellite AOD Observations. We began with AOD retrievals from the two Moderate Resolution Imaging Spectroradiometer (MODIS) instruments onboard the Terra and Aqua satellites and the Multiangle Imaging Spectroradiometer (MISR) instrument onboard Terra. Aerosol retrievals (collection 5) from each MODIS instrument provide near-daily

global coverage of cloud-free regions at a resolution of $10\text{ km} \times 10\text{ km}$.³¹ The MISR retrieval algorithm (version 22) uses multiangle, multispectral observations to provide aerosol optical properties at a spatial resolution of $18\text{ km} \times 18\text{ km}$ and global coverage of cloud-free regions within 9 days.²¹ The operational MODIS and MISR retrievals together provide more reliable global AOD than from either instrument alone.²³

Following van Donkelaar et al.,²³ we collected daily AOD retrievals of these three satellite sensors from 2004 to 2008 and regridded them separately onto a resolution of $0.1^\circ \times 0.1^\circ$. We then divided the world into nine regions with distinct surface type based on the MODIS BRDF/Albedo product (MOD43, Collection 5,³²). We used the available ground-based sun photometer AOD measurements (Aerosol Robotic Network, AERONET,³³) over these regions to identify the average monthly bias of satellite AOD for each region. We retained the daily satellite AOD observations with a local monthly bias less than $\pm 20\%$ or 0.1. We included two textural filters for MODIS AOD to reduce cloud contamination by excluding data with no adjacent retrievals and grids with AOD and coefficient of variation greater than 0.5.^{34,35} These three different (MODIS/Terra, MODIS/Aqua, MISR/Terra) AOD data sets at $0.1^\circ \times 0.1^\circ$ resolution are the major observational inputs for this study.

Inferred PM_{2.5} Chemical Composition from AOD. Our approach to infer the 24-h average ground-level dry PM_{2.5} concentrations of each chemical component, i from the observed aerosol optical depth, AOD_{Sat}, involved a chemical transport model (GEOS-Chem) to calculate that relationship

$$\text{component}_{\text{Sat}}^i = \frac{\text{component}_{\text{CTM}}^i}{\text{AOD}_{\text{CTM}}} \times \text{AOD}_{\text{Sat}} \quad (1)$$

The major PM_{2.5} components included sulfate (SO_4^{2-}), nitrate (NO_3^-), ammonium (NH_4^+), total secondary inorganic aerosols (SIA, sum of SO_4^{2-} , NO_3^- , and NH_4^+ ions), particulate organic mass (OM), black carbon (BC), mineral dust, and sea salt. The subscript CTM indicates values from a chemical transport model. The simulated conversion factor, defined as the ratio of components to AOD, relates the observed AOD to the ground-level PM_{2.5} components. The approach of distributing the observed AOD across simulated aerosol composition has similarity to AOD assimilation methods (e.g., ref 36).

We used the GEOS-Chem global CTM (<http://geos-chem.org>) to calculate the local conversion factors coincident with each satellite observation. The GEOS-Chem model simulates the temporal and three-dimensional spatial distributions of various aerosol components and gases using assimilated meteorology and emission inventories as major inputs [details in the Supporting Information (SI)]. We conducted a global simulation at $2^\circ \times 2.5^\circ$ spatial resolution and three nested regional simulations at $0.5^\circ \times 0.667^\circ$ resolution from 2004 to 2008 using assimilated meteorological data from the Goddard Earth Observing System (GEOS-5) at the NASA Global Modeling Assimilation Office (GMAO). The global simulation outputs are overwritten with nested regional simulations over North America, Europe, and East Asia. The top left panel of Figure 1 provides the boundaries of these regions. These nested simulations improve over the $2^\circ \times 2.5^\circ$ resolution used by van Donkelaar et al.²³ The PM_{2.5} dry mass composition of the lowest layer of the model centered at 70 m above ground was taken to represent the ground-level concentration. We averaged the simulated AOD between 1000 and 1200 h local solar time to correspond with Terra overpass and 1300 and 1500 h local solar

time to correspond with Aqua overpass. We calculated the daily local Terra and Aqua conversion factors as the ratio of 24 h average PM_{2.5} components to the corresponding AOD at satellite overpass period.

We applied eq 1 to produce PM_{2.5} components from individual AOD observations from the two MODIS and the MISR instruments from 2004 to 2008. We accounted for incomplete sampling by scaling the monthly data with the ratio of monthly mean simulated composition sampled continuously versus sampled coincidentally with satellite observations. We capped the variation from the monthly mean simulated composition at the species-dependent uncertainties calculated by van Donkelaar et al.³⁷ This cap represents a level of confidence in the simulation and avoids unrealistic conditions that can arise from the correlation of sensor sampling with PM_{2.5} composition. We required 20 successful satellite observations for each 0.1° grid box per five-year monthly mean; otherwise monthly mean simulated composition was used as occurred for 0.5% of the global population. We averaged the monthly data to obtain the long-term mean satellite-model combined PM_{2.5} composition.

We evaluated the satellite-model estimate with PM_{2.5} composition measurements from networks over North America, Europe, East Asia, and elsewhere with annually representative composition measurements from publications as described in the SI.

The uncertainty associated with the satellite-model PM_{2.5} composition arises from bias in the satellite AOD retrieval, from simulating the PM_{2.5}/AOD ratio, from the simulated PM_{2.5} fractional composition, and from incomplete sampling. We represented the uncertainty in the satellite AOD retrieval bias as the maximum of either an absolute AOD of 0.1 or a relative value of 20%, since AERONET was used to identify and exclude regions and time periods with larger expected bias. We estimated the uncertainty in the model vertical profile bias as the annual mean difference in the PM_{2.5}/AOD ratio if observations from the CALIOP satellite instrument³⁸ were used to adjust the ratio following van Donkelaar et al.³⁷ We assessed the bias in the simulated PM_{2.5} fractional composition for each component (ratio of PM_{2.5} components to total PM_{2.5} mass) by comparison with available in situ observations. Uncertainty due to incomplete sampling was estimated as the difference between the long-term mean simulated PM_{2.5} composition sampled continuously versus coincidentally with the satellite observations. We assumed 100% sampling error for grids without satellite observations. The estimated uncertainty from a quadrature sum of these uncertainty terms may be underestimated since the errors contain systematic components, can be asymmetric, and can be correlated with each other and with PM_{2.5} composition. Thus, we added the median global PM_{2.5} composition to the quadrature sum to better represent the unresolved contributions to total uncertainty especially in the regions with low values of PM_{2.5} composition.

Estimating the PM_{2.5} Emission Sources. PM_{2.5} constituents arise from different emission source sectors such as fossil fuel combustion, biofuel combustion, and biomass burning. Fossil fuel combustion includes burning of coal, oil, and gas from vehicular and industrial sources. Biofuel combustion includes burning of wood and crop residue for domestic cooking and heating. Biomass burning includes both natural open fires and anthropogenic activities such as land clearing and burning in fields. Quantitative determination of these sectoral contributions to PM_{2.5} can inform mitigation strategies.

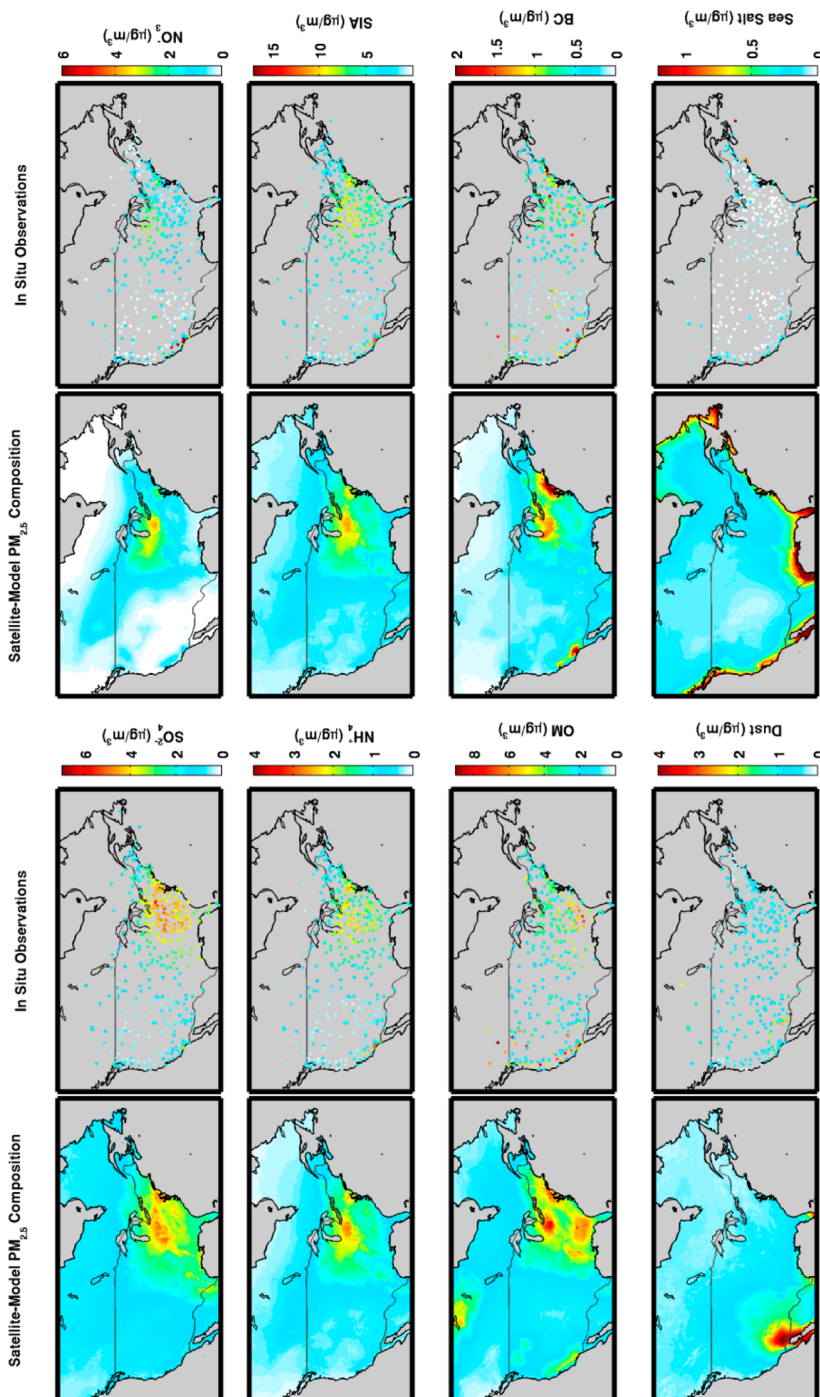


Figure 2. PM_{2.5} composition from satellite-model and in situ observations across North America. PM_{2.5} composition is represented as dry mass. Abbreviations are Secondary Inorganic Aerosol (SIA; the sum of SO₄²⁻, NO₃⁻, and NH₄⁺), Organic Mass (OM), and Black Carbon (BC). Gray denotes water or missing in situ measurement data. Scatter plots are in SI Figure S2.

We therefore estimated the sectoral sources of total PM_{2.5} using sensitivity simulations to exclude specific emission sectors. For this, we performed three global simulations for a year (2005) by excluding fossil fuel combustion, biofuel combustion, and biomass burning sources, respectively. We scaled the PM_{2.5} relative variation from sensitivity simulations (compared with a base simulation) to the sum of satellite-model PM_{2.5} composition estimate. We calculated sectoral contributions of PM_{2.5} at 35% relative humidity to conform with PM_{2.5} measurement standards.

We calculated the regional population exposure for the GBD regions (Global Diseases, Injuries, and Risk Factors 2010 study;

the top panel of Figure 4 shows the 21 GBD regions) using the population data at 0.1 resolution for 2005 described in Brauer et al.³⁹ and the satellite-model PM_{2.5} composition and emission sources.

RESULTS AND DISCUSSION

SI Figure S1 contains a map of the long-term (2004–2008) mean AOD from the MODIS and MISR satellite instruments. Enhancements exist over anthropogenic pollution sources of South and East Asia, over mineral dust source regions of the

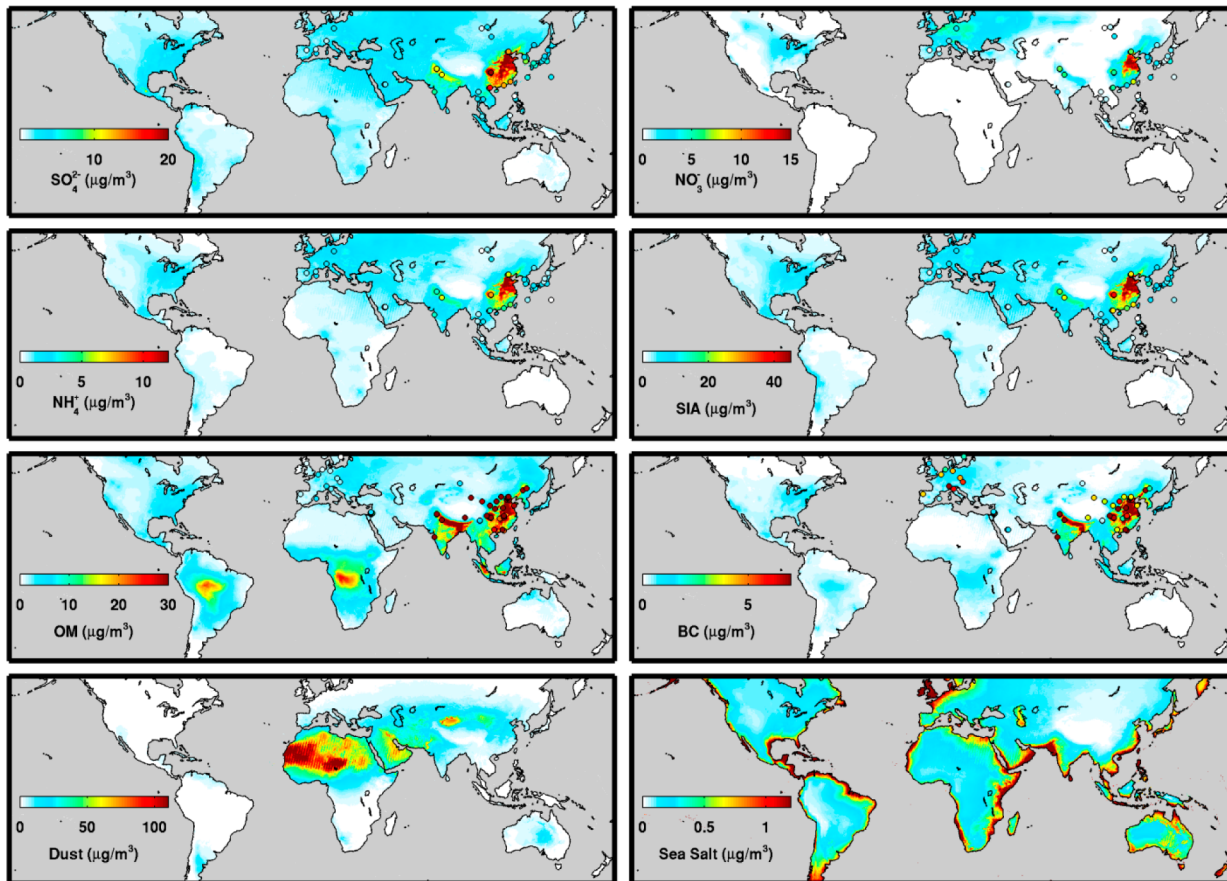


Figure 3. Satellite-model global long-term mean (2004–2008) $\text{PM}_{2.5}$ composition. $\text{PM}_{2.5}$ composition is represented as dry mass. Abbreviations are Secondary Inorganic Aerosol (SIA; the sum of SO_4^{2-} , NO_3^- , and NH_4^+), Organic Mass (OM), and Black Carbon (BC). Gray denotes water. Values from in situ observations are overlaid as colored circles. SI Table S1 contains the detailed comparison statistics.

Sahara, and over biomass burning regions of South America, Central Africa, and Equatorial and Southeast Asia.

Figure 1 shows the long-term (2004–2008) mean GEOS-Chem simulated ratio of $\text{PM}_{2.5}$ components to AOD. The ratio represents the relative importance of various $\text{PM}_{2.5}$ components to the total AOD over different regions of the globe. The mass/AOD ratio is high over regions with relatively large abundance of that $\text{PM}_{2.5}$ component near the ground. Nonhygroscopic components (e.g., mineral dust) exhibit high conversion factors due to the low contribution of aerosol water to AOD. The high mass/AOD ratios for secondary inorganic $\text{PM}_{2.5}$, OM, and mineral dust indicate that these components are the dominant contributors to global AOD over land. Secondary inorganic $\text{PM}_{2.5}$ dominates over industrial regions. Particulate organic mass from biomass burning is the primary contributor to AOD over the Amazon, Central Africa, Northern India, and Oceania. Mineral dust is the primary contributor to AOD over deserts. Black carbon is a small component of AOD but is more apparent in local hotspots. Sea salt generally has the lowest conversion factor over land.

Figure 2 shows the satellite-model and in situ observations of North American $\text{PM}_{2.5}$ composition. The in situ observation of a large sulfate burden in the East is well reproduced in the satellite-model product. Nitrate and ammonium are enhanced south of the Great Lakes where intense agriculture sources of ammonia and weak sulfur sources contribute to excess ammonia gas that is available for forming ammonium nitrate. The Californian nitrate enhancements are under-predicted reflecting difficulties in

representing this heterogeneous region.^{40,41} Together these secondary inorganic ions comprise a major fraction of the total $\text{PM}_{2.5}$ in the Eastern U.S., reaching concentrations of approximately $10 \mu\text{g}/\text{m}^3$. The spatial pattern of particulate organic mass over the southeastern U.S. is generally captured in the satellite-model product. Black carbon concentrations exhibit hotspots in industrial regions; performance elsewhere is more variable given the stochastic nature of fires. Fine-mode dust and fine sea salt emissions are weak contributors to $\text{PM}_{2.5}$ mass throughout the continent with typical mass concentrations below $1 \mu\text{g}/\text{m}^3$. The primary exception is for mineral dust over deserts in the southwest.

SI Figure S2 shows scatter plots of satellite-model $\text{PM}_{2.5}$ components with North American in situ observations, and SI Table S1 contains detailed comparison statistics of in situ with either the satellite-model or pure GEOS-Chem $\text{PM}_{2.5}$ composition. The correlation between satellite-model sulfate and ground monitors is high ($r = 0.95$, slope = 0.89). Concentrations are also well predicted for nitrate ($r = 0.68$, slope = 1.01) and ammonium ($r = 0.89$, slope = 0.98). The performance for OM is weaker ($r = 0.45$, slope = 1.17) likely due to the difficulty in simulating secondary organic aerosol and fires and due to sporadic measurements of stochastic fire events. Black carbon, mineral dust, and sea salt have modest agreement with in situ measurements with correlations of 0.56, 0.58, and 0.62, respectively. The bias for all components is within 35%. The in situ observations are similarly correlated with the satellite-model product and the GEOS-Chem simulation, with noteworthy

Table 1. Population-Weighted Regional PM_{2.5} Composition and Three Major Emission Sources Contributing to PM_{2.5}^a

| region | PM _{2.5} composition ($\mu\text{g}/\text{m}^3$) | | | | | | | | PM _{2.5} emission ($\mu\text{g}/\text{m}^3$) | | | population (%) |
|------------------------------|--|------------------------------|------------------------------|------|------|-----|------|---------|---|---------|---------|----------------|
| | SO ₄ ²⁻ | NO ₃ ⁻ | NH ₄ ⁺ | SIA | OM | BC | dust | seasalt | fossil fuel | biofuel | biomass | |
| World | 6.2 | 2.2 | 2.7 | 11.1 | 11.9 | 2.5 | 11.1 | 0.6 | 17.1 | 11.2 | 1.3 | 100.0 |
| Asia Pacific, High Income | 5.5 | 1.5 | 2.0 | 9.0 | 4.8 | 1.9 | 3.7 | 0.9 | 16.2 | 2.1 | 0.3 | 2.7 |
| Asia, Central | 3.2 | 0.6 | 1.3 | 5.1 | 3.7 | 0.5 | 21.3 | 0.1 | 7.2 | 6.5 | 0.3 | 1.3 |
| Asia, East | 14.5 | 6.6 | 7.0 | 28.0 | 21.7 | 5.7 | 11.7 | 0.5 | 45.8 | 20.2 | 0.3 | 21.2 |
| Asia, South | 6.9 | 1.1 | 2.8 | 10.8 | 21.6 | 3.9 | 14.3 | 0.5 | 15.8 | 24.1 | 0.6 | 22.9 |
| Asia, South East | 3.6 | 0.2 | 1.1 | 5.0 | 8.0 | 1.2 | 1.6 | 1.0 | 6.7 | 5.4 | 3.2 | 8.7 |
| Australasia | 0.7 | 0.1 | 0.2 | 1.0 | 0.8 | 0.1 | 1.1 | 1.0 | 1.1 | 0.2 | 0.2 | 0.4 |
| Caribbean | 1.2 | 0.2 | 0.2 | 1.6 | 1.0 | 0.2 | 4.8 | 1.7 | 1.8 | 0.1 | 0.2 | 0.5 |
| Europe, Central | 3.8 | 3.6 | 2.5 | 9.9 | 4.1 | 0.8 | 3.2 | 0.3 | 13.7 | 4.4 | 0.2 | 1.9 |
| Europe, Eastern | 2.9 | 2.3 | 1.7 | 6.9 | 2.9 | 0.4 | 2.8 | 0.2 | 9.0 | 2.8 | 0.3 | 3.3 |
| Europe, Western | 2.3 | 3.2 | 1.7 | 7.2 | 2.1 | 0.7 | 3.3 | 0.8 | 10.6 | 1.4 | 0.2 | 6.1 |
| Latin America, Andean | 2.1 | 0.0 | 0.6 | 2.7 | 3.2 | 0.2 | 0.1 | 0.5 | 2.8 | 0.6 | 2.9 | 0.8 |
| Latin America, Central | 3.1 | 0.4 | 1.0 | 4.4 | 2.5 | 0.5 | 1.6 | 0.7 | 5.2 | 0.4 | 1.4 | 3.4 |
| Latin America, Southern | 1.9 | 0.1 | 0.5 | 2.4 | 2.7 | 0.3 | 2.4 | 0.5 | 3.0 | 1.2 | 1.0 | 0.9 |
| Latin America, Tropical | 1.1 | 0.1 | 0.4 | 1.6 | 3.4 | 0.3 | 0.2 | 0.6 | 2.1 | 1.6 | 1.8 | 2.9 |
| North Africa/Middle East | 3.5 | 0.3 | 1.2 | 4.9 | 1.7 | 0.4 | 29.0 | 0.6 | 6.7 | 0.8 | 0.2 | 6.4 |
| North America, High Income | 2.9 | 1.3 | 1.3 | 5.6 | 3.9 | 0.9 | 0.7 | 0.4 | 10.2 | 0.5 | 0.2 | 5.0 |
| Oceania | 0.5 | 0.0 | 0.1 | 0.6 | 0.2 | 0.0 | 0.1 | 0.5 | 0.1 | 0.1 | 0.1 | 0.1 |
| Sub-Saharan Africa, Central | 1.6 | 0.0 | 0.5 | 2.1 | 14.8 | 0.8 | 4.9 | 0.3 | 1.3 | 3.9 | 14.4 | 1.3 |
| Sub-Saharan Africa, East | 1.1 | 0.1 | 0.3 | 1.4 | 4.6 | 0.5 | 9.2 | 0.6 | 1.0 | 3.7 | 2.7 | 4.8 |
| Sub-Saharan Africa, Southern | 1.9 | 0.1 | 0.6 | 2.6 | 3.4 | 0.3 | 0.7 | 0.6 | 3.2 | 0.9 | 2.8 | 1.0 |
| Sub-Saharan Africa, West | 1.5 | 0.1 | 0.5 | 2.1 | 5.1 | 0.4 | 45.7 | 0.3 | 2.4 | 2.5 | 5.4 | 4.4 |

^aThe top panel of Figure 4 shows the borders of GBD (Global Diseases, Injuries, and Risk Factors 2010 study) regions. Abbreviations are Secondary Inorganic Aerosol (SIA; the sum of SO₄²⁻, NO₃⁻, and NH₄⁺), Organic Mass (OM), and Black Carbon (BC).

improvements in the slope versus the GEOS-Chem simulation for secondary inorganic ions.

Figure 3 shows the global satellite-model estimate of long-term mean PM_{2.5} composition where the filled circles represent the location and value of the in situ observations used to evaluate the data set outside of North America. Detailed statistics are given in SI Table S1. Secondary inorganic aerosol concentrations over East China exceed 30 $\mu\text{g}/\text{m}^3$. About half of the simulated secondary inorganic aerosol is sulfate which is consistent with in situ measurements.⁴² The Indo-Gangetic Plain, China, and biomass burning regions of South America and Central Africa are highlighted in the OM map. Previous studies have also noted pronounced OM in these regions.^{43,44} Hotspots of black carbon are most apparent in China and the Indo-Gangetic Plain where in situ measurements also indicate enhancements.^{44,45} Mineral dust is the largest contributor to PM_{2.5} over the desert regions of North Africa, Middle East, and Central Asia with concentrations greater than 50 $\mu\text{g}/\text{m}^3$ over broad regions. The satellite-model product exhibits high correlations for secondary inorganic aerosol ($r = 0.93$) and its components, with slopes within 20% of unity. Carbonaceous aerosols are again less well represented; sparse in situ monitors may play a role for fires. The satellite-model product outperforms the pure model simulation for all components (e.g., for secondary inorganic aerosols the slope improved from 0.64 to 0.91; for organic matter the correlation improved from 0.61 to 0.67).

Table 1 summarizes the global and regional statistics of population exposure to ambient PM_{2.5} composition. Our estimates suggest that particulate organic mass is the dominant form of ambient PM_{2.5} with a global population-weighted concentration of 12 $\mu\text{g}/\text{m}^3$. Other major contributors to global population-weighted PM_{2.5} mass are secondary inorganic components (11 $\mu\text{g}/\text{m}^3$) and mineral dust (11 $\mu\text{g}/\text{m}^3$). The secondary inorganic components are dominated by sulfate (6.2

$\mu\text{g}/\text{m}^3$), followed by ammonium (2.7 $\mu\text{g}/\text{m}^3$) and nitrate (2.2 $\mu\text{g}/\text{m}^3$). On a regional scale, secondary inorganic PM_{2.5} concentrations are noteworthy in East Asia (28 $\mu\text{g}/\text{m}^3$) and South Asia (11 $\mu\text{g}/\text{m}^3$). The mean ambient particulate organic mass concentration is 22 $\mu\text{g}/\text{m}^3$ in both South Asia and East Asia. Mineral dust concentrations exceed 20 $\mu\text{g}/\text{m}^3$ in West Africa, North Africa, Middle East, and Central Asia. These PM_{2.5} values are higher than previous work^{18,23} arising from our use of satellite AOD for all fine mode fraction values and increased carbonaceous aerosol emissions over East Asia as described in the SI.

SI Figure S3 shows the total estimated absolute uncertainty of the satellite-model PM_{2.5} composition as determined by propagation of error. For many species, the primary source of uncertainty arose from the simulated PM_{2.5} fractional composition with corresponding values for sulfate (27%), nitrate (38%), ammonium (29%), SIA (29%), OM (45%), BC (36%), dust (52%), and sea salt (122%). In regions of low AOD (below 0.1), uncertainty in the satellite AOD retrieval can exceed 100%. Uncertainty due to model vertical profile bias was 10–30% in most regions with exceptions in convective regions (SI Figure S4). However, uncertainty on a monthly basis could be even higher due to seasonal differences in vertical mixing.⁴⁶ Sampling uncertainty was below 30% throughout low latitudes except for seasonally convective regions with cloud cover that prohibits observations (SI Figure S5). Decreases in observation frequency at high latitudes increased uncertainty from incomplete sampling especially for nitrate and carbonaceous components that have large seasonal variation. The global population-weighted mean uncertainty for sulfate (2.8 $\mu\text{g}/\text{m}^3$), nitrate (1.2 $\mu\text{g}/\text{m}^3$), ammonium (1.2 $\mu\text{g}/\text{m}^3$), secondary inorganic PM_{2.5} (5.0 $\mu\text{g}/\text{m}^3$), organic mass (7.3 $\mu\text{g}/\text{m}^3$), black carbon (1.2 $\mu\text{g}/\text{m}^3$), mineral dust (7.9 $\mu\text{g}/\text{m}^3$), and sea salt (0.8 $\mu\text{g}/\text{m}^3$) ranged from ~45% of the population-weighted concentrations for many species (Table 1) to ~142% for sea salt.

Figure 4 shows the contributions to PM_{2.5} from fossil fuel combustion, biofuel combustion, and biomass burning.

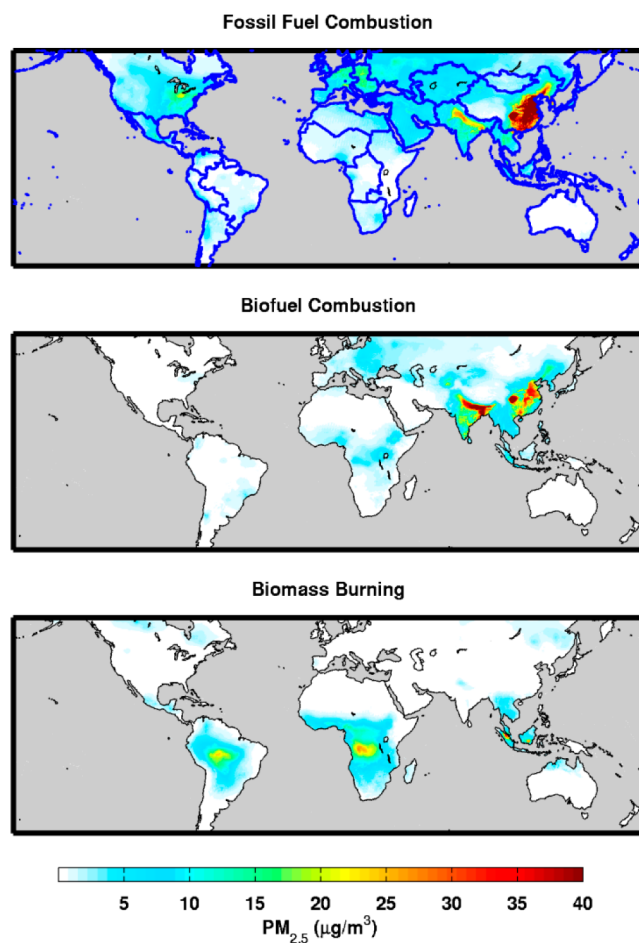


Figure 4. Estimate of three major emission sources contributing to PM_{2.5}. Gray denotes water. The thick border lines in the top panel represent the GBD (Global Diseases, Injuries, and Risk Factors 2010 study) regions.

Enhanced anthropogenic sources are apparent over industrial and populated regions. Biofuel sources over Asia reflect domestic cooking and heating with nonfossil fuel sources. Biomass burning dominates in Central Africa and the Amazon. Biogenic sources, mineral dust, and sea salt constitute the remaining portion of PM_{2.5}. Table 1 contains the global and regional statistics of population exposure to various source sectors of PM_{2.5}. Population-weighted PM_{2.5} is dominated by fossil fuel combustion (17 µg/m³) followed by biofuel combustion (11 µg/m³) and biomass burning (1.3 µg/m³). PM_{2.5} is high from emissions of fossil fuel combustion over East Asia (46 µg/m³), biofuel combustion over South Asia (24 µg/m³) and East Asia (20 µg/m³), and biomass burning over Central Africa (14 µg/m³). Although these sensitivity simulations are uncertain, it is noteworthy that outdoor PM_{2.5} from biofuel combustion is comparable to that from fossil fuel combustion in South Asia. This is in line with previous findings of high ambient PM_{2.5} exposure from biofuel burning^{47,48} and in addition to PM_{2.5} exposure from household air pollution.⁴⁹

The chemical composition of ambient ground-level fine particulate mass is of relevance for epidemiological and health impact studies.^{50–53} To our knowledge, these estimates developed from satellite AOD observations and CTM

simulations offer the first assessment of the long-term exposure to all major PM_{2.5} chemical components throughout the world. Multiple opportunities exist to improve the estimates. Advances in satellite remote sensing⁵⁴ could yield more observational information on aerosol components. Future developments in the modeling of aerosol composition such as organic mass are needed. Other emerging sources of information on the sources of aerosol precursors include satellite observations of trace gases⁵⁵ such as NO₂, SO₂,⁵⁷ and NH₃.⁵⁸ Assimilation of these components into a chemical transport model would provide additional constraints on PM_{2.5} composition. Finer resolution satellite retrievals and simulations would better resolve intra-urban gradients. Trace metals are an important PM_{2.5} component that should be added as their simulation capability improves.

ASSOCIATED CONTENT

Supporting Information

Descriptions of the GEOS-Chem model, in situ data, five figures, and two tables. This material is available free of charge via the Internet at <http://pubs.acs.org>.

AUTHOR INFORMATION

Corresponding Author

*Phone: 19024941820. Fax: 19024945191. E-mail: philip.sajeev@dal.ca.

Notes

The authors declare no competing financial interest.

ACKNOWLEDGMENTS

This work was supported by Health Canada, the Natural Sciences and Engineering Research Council of Canada, and the U.S. National Institutes of Health. Sajeev Philip was supported by an ACEnet Fellowship. Computational facilities are partially provided by ACEnet, the regional high performance computing consortium for universities in Atlantic Canada. We are grateful to the MODIS, MISR, CALIOP, AERONET, NAPS, CAPMoN, CASTNET, IMPROVE, EPA-AQS, EMEP, and EANET teams for making their data publicly available.

REFERENCES

- Bell, M. L.; Ebisu, K.; Peng, R. D.; Samet, J. M.; Dominici, F. Hospital admissions and chemical composition of fine particle air pollution. *Am. J. Respir. Crit. Care Med.* **2009**, *179* (12), 1115–1120 DOI: 10.1164/rccm.200808-1240OC.
- Ito, K.; Mathes, R.; Ross, Z.; Nadas, A.; Thurston, G.; Matte, T. Fine particulate matter constituents associated with cardiovascular hospitalizations and mortality in New York City. *Environ. Health Perspect.* **2011**, *119* (4), 467–473 DOI: 10.1289/ehp.1002667.
- Kim, S.; Peel, J. L.; Hannigan, M. P.; Dutton, S. J.; Sheppard, L.; Clark, M. L.; Vedral, S. The temporal lag structure of short-term associations of fine particulate matter chemical constituents and cardiovascular and respiratory hospitalizations. *Environ. Health Perspect.* **2012**, *120* (8), 1094–1099 DOI: 10.1289/ehp.1104721.
- Burnett, R. T.; Brook, J.; Dann, T.; Delocla, C.; Philips, O.; Cakmak, S.; Vincent, R.; Goldberg, M. S.; Krewski, D. Association between particulate- and gas-phase components of urban air pollution and daily mortality in eight Canadian cities. *Inhalation Toxicol.* **2000**, *12*, 15–39 DOI: 10.1080/08958370050164851.
- Ostro, B.; Lipsett, M.; Reynolds, P.; Goldberg, D.; Hertz, A.; Garcia, C.; Henderson, K. D.; Bernstein, L. Long-term exposure to constituents of fine particulate air pollution and mortality: results from the California teachers study. *Environ. Health Perspect.* **2010**, *118* (3), 363–369 DOI: 10.1289/ehp.0901181.

- (6) Zhou, J.; Ito, K.; Lall, R.; Lippmann, M.; Thurston, G. Time-series analysis of mortality effects of fine particulate matter components in Detroit and Seattle. *Environ. Health Perspect.* **2011**, *119* (4), 461–466 DOI: 10.1289/ehp.1002613.
- (7) Cao, J.; Xu, H.; Xu, Q.; Chen, B.; Kan, H. Fine particulate matter constituents and cardiopulmonary mortality in a heavily polluted Chinese city. *Environ. Health Perspect.* **2012**, *120* (3), 373–378 DOI: 10.1289/ehp.1103671.
- (8) Son, J.; Lee, J.; Kim, K.; Jung, K.; Bell, M. L. Characterization of fine particulate matter and associations between particulate chemical constituents and mortality in Seoul, Korea. *Environ. Health Perspect.* **2012**, *120* (6), 872–878 DOI: 10.1289/ehp.1104316.
- (9) Pope, C. A.; Ezzati, M.; Dockery, D. W. Fine-particulate air pollution and life expectancy in the United States. *N. Engl. J. Med.* **2009**, *360* (4), 376–386 DOI: 10.1056/NEJMoa0805646.
- (10) Brook, R. D.; Rajagopalan, S.; Pope, C. A.; Brook, J. R.; Bhatnagar, A.; Diez-Roux, A. V.; Holguin, F.; Hong, Y.; Luepker, R. V.; Mittleman, M. A.; Peters, A.; Siscovick, D.; Smith, S. C.; Whitsel, L.; Kaufman, J. D.; American Heart Association Council on Epidemiology and Prevention; Council on the Kidney in Cardiovascular Disease; Council on Nutrition, Physical Activity and Metabolism. Particulate matter air pollution and cardiovascular disease: an update to the scientific statement from the American Heart Association. *Circulation* **2010**, *121* (21), 2331–2378 DOI: 10.1161/CIR.0b013e3181dbece1.
- (11) Lepeule, J.; Laden, F.; Dockery, D.; Schwartz, J. Chronic exposure to fine particles and mortality: an extended follow-up of the Harvard six cities study from 1974 to 2009. *Environ. Health Perspect.* **2012**, *120* (7), 965–970 DOI: 10.1289/ehp.1104660.
- (12) Martin, R. V. Satellite remote sensing of surface air quality. *Atmos. Environ.* **2008**, *42* (34), 7823784310.1016/j.atmosenv.2008.07.018.
- (13) Hoff, R. M.; Christopher, S. A. Remote sensing of particulate pollution from space: have we reached the promised land? *J. Air Waste Manage. Assoc.* **2009**, *59* (6), 645–675 DOI: 10.3155/1047-3289.59.6.645.
- (14) Wang, J.; Christopher, S. A. Intercomparison between satellite-derived aerosol optical thickness and PM_{2.5} mass: Implications for air quality studies. *Geophys. Res. Lett.* **2003**, *30* (21), 2095 DOI: 10.1029/2003GL018174.
- (15) Engel-Cox, J. A.; Holloman, C. H.; Coutant, B. W.; Hoff, R. M. Qualitative and quantitative evaluation of MODIS satellite sensor data for regional and urban scale air quality. *Atmos. Environ.* **2004**, *38* (16), 2495–2509 DOI: 10.1016/j.atmosenv.2004.01.039.
- (16) Kloog, I.; Koutrakis, P.; Coull, B. A.; Lee, H. J.; Schwartz, J. Assessing temporally and spatially resolved PM_{2.5} exposures for epidemiological studies using satellite aerosol optical depth measurements. *Atmos. Environ.* **2011**, *45* (35), 6267–6275 DOI: 10.1016/j.atmosenv.2011.08.066.
- (17) Al-Saadi, J.; Szykman, J.; Pierce, R. B.; Kittaka, C.; Neil, D.; Chu, D. A.; Remer, L.; Gumley, L.; Prins, E.; Weinstock, L.; MacDonald, C.; Wayland, R.; Dimmick, F.; Fishman, J. Improving national air quality forecasts with satellite aerosol observations. *Bull. Am. Meteorol. Soc.* **2005**, *86* (9), 1249–1261 DOI: 10.1175/BAMS-86-9-1249.
- (18) van Donkelaar, A.; Martin, R. V.; Pasch, A. N.; Szykman, J. J.; Zhang, L.; Wang, Y. X.; Chen, D. Improving the accuracy of daily satellite-derived ground-level fine aerosol concentration estimates for North America. *Environ. Sci. Technol.* **2012**, *46* (21), 11971–11978 DOI: 10.1021/es3025319.
- (19) Paciorek, C. J.; Liu, Y. Limitations of remotely sensed aerosol as a spatial proxy for fine particulate matter. *Environ. Health Perspect.* **2009**, *117* (6), 904–909 DOI: 10.1289/ehp.0800360.
- (20) Liu, Y.; Koutrakis, P.; Kahn, R. Estimating fine particulate matter component concentrations and size distributions using satellite-retrieved fractional aerosol optical depth: part 1 - method development. *J. Air Waste Manage. Assoc.* **2007**, *57* (11), 1351–1359 DOI: 10.3155/1047-3289.S7.11.1351.
- (21) Kahn, R. A.; Li, W.-H.; Moroney, C.; Diner, D. J.; Martonchik, J. V.; Fishbein, E. Aerosol source plume physical characteristics from space-based multiangle imaging. *J. Geophys. Res.: Atmos.* **2007**, *112* (D11), D11205 DOI: 10.1029/2006JD007647.
- (22) Liu, Y.; Park, R. J.; Jacob, D. J.; Li, Q. B.; Kilaru, V.; Sarnat, J. A. Mapping annual mean ground-level PM_{2.5} concentrations using multiangle imaging spectroradiometer aerosol optical thickness over the contiguous United States. *J. Geophys. Res.: Atmos.* **2004**, *109* (D22), D22206 DOI: 10.1029/2004JD005025.
- (23) van Donkelaar, A.; Martin, R. V.; Brauer, M.; Kahn, R.; Levy, R.; Verduzco, C.; Villeneuve, P. J. Global estimates of ambient fine particulate matter concentrations from satellite-based aerosol optical depth: development and application. *Environ. Health Perspect.* **2010**, *118* (6), 847–855 DOI: 10.1289/ehp.0901623.
- (24) Wang, Z. S.; Chien, C.; Tonnesen, G. S. Development of a tagged species source apportionment algorithm to characterize three-dimensional transport and transformation of precursors and secondary pollutants. *J. Geophys. Res.: Atmos.* **2009**, *114*, D21206 DOI: 10.1029/2008JD010846.
- (25) Anenberg, S. C.; Talgo, K.; Arunachalam, S.; Dolwick, P.; Jang, C.; West, J. J. Impacts of global, regional, and sectoral black carbon emission reductions on surface air quality and human mortality. *Atmos. Chem. Phys.* **2011**, *11* (14), 7253–7267 DOI: 10.5194/acp-11-7253-2011.
- (26) Malm, W. C.; Sisler, J. F.; Huffman, D.; Eldred, R. A.; Cahill, T. A. Spatial and seasonal trends in particle concentration and optical extinction in the United States. *J. Geophys. Res.: Atmos.* **1994**, *99* (D1), 1347–1370 DOI: 10.1029/93JD02916.
- (27) Dabek-Zlotorzynska, E.; Dann, T. F.; Martinelango, P. K.; Celo, V.; Brook, J. R.; Mathieu, D.; Ding, L.; Austin, C. C. Canadian National Air Pollution Surveillance (NAPS) PM_{2.5} speciation program: methodology and PM_{2.5} chemical composition for the years 2003–2008. *Atmos. Environ.* **2011**, *45* (3), 673–686 DOI: 10.1016/j.atmosenv.2010.10.024.
- (28) Bell, M. L.; Dominici, F.; Ebisu, K.; Zeger, S. L.; Samet, J. M. Spatial and temporal variation in PM_{2.5} chemical composition in the United States for health effects studies. *Environ. Health Perspect.* **2007**, *115* (7), 989–995 DOI: 10.1289/ehp.9621.
- (29) Hand, J. L.; Schichtel, B. A.; Pitchford, M.; Malm, W. C.; Frank, N. H. Seasonal composition of remote and urban fine particulate matter in the United States. *J. Geophys. Res.: Atmos.* **2012**, *117*, D05209 DOI: 10.1029/2011JD017122.
- (30) Hand, J. L. et al. *IMPROVE (Interagency Monitoring of Protected Visual Environments): Spatial and seasonal patterns and temporal variability of haze and its constituents in the United States*; Report V; Cooperative Institute for Research in the Atmosphere: Fort Collins, CO, 2011.
- (31) Levy, R. C.; Remer, L. A.; Mattoo, S.; Vermote, E. F.; Kaufman, Y. J. Second-generation operational algorithm: Retrieval of aerosol properties over land from inversion of Moderate Resolution Imaging Spectroradiometer spectral reflectance. *J. Geophys. Res.: Atmos.* **2007**, *112* (D13), D13211 DOI: 10.1029/2006JD007811.
- (32) Schaaf, C. B.; Gao, F.; Strahler, A. H.; Lucht, W.; Li, X. W.; Tsang, T.; Strugnell, N. C.; Zhang, X. Y.; Jin, Y. F.; Muller, J. P.; Lewis, P.; Barnsley, M.; Hobson, P.; Disney, M.; Roberts, G.; Dunderdale, M.; Doll, C.; d'Entremont, R. P.; Hu, B. X.; Liang, S. L.; Privette, J. L.; Roy, D. First operational BRDF, albedo nadir reflectance products from MODIS. *Remote Sens. Environ.* **2002**, *83* (1–2), 135–148 PII S0034-4257(02)00091-3; DOI: 10.1016/S0034-4257(02)00091-3.
- (33) Holben, B. N.; Eck, T. F.; Slutsker, I.; Tanre, D.; Buis, J. P.; Setzer, A.; Vermote, E.; Reagan, J. A.; Kaufman, Y. J.; Nakajima, T.; Lavenu, F.; Jankowiak, I.; Smirnov, A. AERONET - A federated instrument network and data archive for aerosol characterization. *Remote Sens. Environ.* **1998**, *66* (1), 1–16 DOI: 10.1016/S0034-4257(98)00031-5.
- (34) Zhang, J.; Reid, J. S. MODIS aerosol product analysis for data assimilation: assessment of over-ocean level 2 aerosol optical thickness retrievals. *J. Geophys. Res.* **2006**, *111*, D22207 DOI: 10.1029/2005JD006898.
- (35) Hyer, E. J.; Reid, J. S.; Zhang, J. An over-land aerosol optical depth data set for data assimilation by filtering, correction, and aggregation of MODIS Collection 5 optical depth retrievals. *Atmos. Meas. Tech.* **2011**, *4* (3), 379–408 DOI: 10.5194/amt-4-379-2011.
- (36) Saide, P. E.; Carmichael, G. R.; Liu, Z.; Schwartz, C. S.; Lin, H. C.; da Silva, A. M.; Hyer, E. Aerosol optical depth assimilation for a size-resolved sectional model: impacts of observationally constrained, multi-

- wavelength and fine mode retrievals on regional scale analyses and forecasts. *Atmos. Chem. Phys.* **2013**, *13* (20), 10425–10444 DOI: 10.5194/acp-13-10425-2013.
- (37) van Donkelaar, A.; Martin, R. V.; Spurr, R. J. D.; Drury, E.; Remer, L. A.; Levy, R. C.; Wang, J. Optimal estimation for global ground-level fine particulate matter concentrations. *J. Geophys. Res.: Atmos.* **2013**, *118* (11), 5621–5636 DOI: 10.1002/jgrd.50479.
- (38) Winker, D. M.; Hunt, W. H.; McGill, M. J. Initial performance assessment of CALIOP. *Geophys. Res. Lett.* **2007**, *34* (19), L19803 DOI: 10.1029/2007GL030135.
- (39) Brauer, M.; Amann, M.; Burnett, R. T.; Cohen, A.; Dentener, F.; Ezzati, M.; Henderson, S. B.; Krzyzanowski, M.; Martin, R. V.; Van Dingenen, R.; van Donkelaar, A.; Thurston, G. D. Exposure assessment for estimation of the global burden of disease attributable to outdoor air pollution. *Environ. Sci. Technol.* **2012**, *46* (2), 652–660 DOI: 10.1021/es2025752.
- (40) Walker, J. M.; Philip, S.; Martin, R. V.; Seinfeld, J. H. Simulation of nitrate, sulfate, and ammonium aerosols over the United States. *Atmos. Chem. Phys.* **2012**, *12* (22), 11213–11227 DOI: 10.5194/acp-12-11213-2012.
- (41) Heald, C. L.; Collett, J. L., Jr.; Lee, T.; Benedict, K. B.; Schwandner, F. M.; Li, Y.; Clarisse, L.; Hurtmans, D. R.; Van Damme, M.; Clerbaux, C.; Coheur, P.-F.; Philip, S.; Martin, R. V.; Pye, H. O. T. Atmospheric ammonia and particulate inorganic nitrogen over the United States. *Atmos. Chem. Phys.* **2012**, *12* (21), 10295–10312 DOI: 10.5194/acp-12-10295-2012.
- (42) Yang, F.; Tan, J.; Zhao, Q.; Du, Z.; He, K.; Ma, Y.; Duan, F.; Chen, G.; Zhao, Q. Characteristics of PM_{2.5} speciation in representative megacities and across China. *Atmos. Chem. Phys.* **2011**, *11* (11), 5207–5219 DOI: 10.5194/acp-11-5207-2011.
- (43) Chowdhury, M. *Characterization of fine particle air pollution in the Indian subcontinent*. Ph.D. Thesis, Georgia Institute of Technology, USA, 2004.
- (44) Fu, T.-M.; Cao, J. J.; Zhang, X. Y.; Lee, S. C.; Zhang, Q.; Han, Y. M.; Qu, W. J.; Han, Z.; Zhang, R.; Wang, Y. X.; Chen, D.; Henze, D. K. Carbonaceous aerosols in China: top-down constraints on primary sources and estimation of secondary contribution. *Atmos. Chem. Phys.* **2012**, *12* (5), 2725–2012 DOI: 10.5194/acp-12-2725-2012.
- (45) Hopke, P. K.; Cohen, D. D.; Begum, B. A.; Biswas, S. K.; Ni, B.; Pandit, G. G.; Santoso, M.; Chung, Y.; Davy, P.; Markowitz, A.; Waheed, S.; Siddique, N.; Santos, F. L.; Pabroa, P. C. B.; Seneviratne, M. C. S.; Wimolwattanapun, W.; Bunrapob, S.; Vuong, T. B.; Duy Hien, P.; Markowicz, A. Urban air quality in the Asian region. *Sci. Total Environ.* **2008**, *404* (1), 103–112 http://dx.doi.org/10.1016/j.scitotenv.2008.05.039.
- (46) Ford, B.; Heald, C. L. An A-train and model perspective on the vertical distribution of aerosols and CO in the Northern Hemisphere. *J. Geophys. Res.: Atmos.* **2012**, *117*, D06211 DOI: 10.1029/2011JD016977.
- (47) Lim, S. S.; Vos, T.; Flaxman, A. D.; Danaei, G. A comparative risk assessment of burden of disease and injury attributable to 67 risk factors and risk factor clusters in 21 regions, 1990–2010: a systematic analysis for the Global Burden of Disease Study 2010. *Lancet* **2012**, *380* (9859), 2224–2260.
- (48) Stone, E.; Schauer, J.; Quraishi, T. A.; Mahmood, A. Chemical characterization and source apportionment of fine and coarse particulate matter in Lahore, Pakistan. *Atmos. Environ.* **2010**, *44* (8), 1062–1070 DOI: 10.1016/j.atmosenv.2009.12.015.
- (49) Balakrishnan, K.; Ghosh, S.; Ganguli, B.; Sambandam, S.; Bruce, N.; Barnes, D.; Smith, K. State and national household concentrations of PM_{2.5} from solid cookfuel use: results from measurements and modeling in India for estimation of the global burden of disease. *Environ. Health* **2013**, *12* (1), 77.
- (50) Health Effects Institute Understanding the Health Effects of Components of the Particulate Matter Mix: Progress and Next Steps. 2004.
- (51) National Research Council Research Priorities for Airborne Particulate Matter: IV. Continuing Research Progress. Committee on Research Priorities for Airborne Particulate Matter. National Academies Press: Washington, DC, 2004.
- (52) Bell, M. L.; HEI Health Review Committee. Assessment of the health impacts of particulate matter characteristics. *Res. Rep. - Health Eff. Inst.* **2012**, No. 161, 5–38.
- (53) U.S. EPA. *Integrated Science Assessment for Particulate Matter (Final Report)*; EPA/600/R-08/139F; U.S. Environmental Protection Agency: Washington, DC, 2009.
- (54) Mishchenko, M. I.; Cairns, B.; Kopp, G.; Schueler, C. F.; Fafaul, B. A.; Hansen, J. E.; Hooker, R. J.; Itchkawich, T.; Maring, H. B.; Travis, L. D. Accurate monitoring of terrestrial aerosols and total solar irradiance - Introducing the glory mission. *Bull. Am. Meteorol. Soc.* **2007**, *88* (5), 677–691 DOI: 10.1175/BAMS-88-5-677.
- (55) Streets, D. G.; Canty, T.; Carmichael, G. R.; de Foy, B.; Dickerson, R. R.; Duncan, B. N.; Edwards, D. P.; Haynes, J. A.; Henze, D. K.; Houyoux, M. R.; Jacob, D. J.; Krotkov, N. A.; Lamsal, L. N.; Liu, Y.; Lu, Z.; Martin, R. V.; Pfister, G. G.; Pinder, R. W.; Salawitch, R. J.; Wecht, K. J. Emissions estimation from satellite retrievals: a review of current capability. *Atmos. Environ.* **2013**, *77* (0), 1011–1042 http://dx.doi.org/10.1016/j.atmosenv.2013.05.051.
- (56) Boersma, K. F.; Eskes, H. J.; Dirksen, R. J.; van der A, R. J.; Vreekind, J. P.; Stammes, P.; Huijnen, V.; Kleipool, Q. L.; Sneep, M.; Claas, J.; Leitao, J.; Richter, A.; Zhou, Y.; Brunner, D. An improved tropospheric NO₂ column retrieval algorithm for the Ozone Monitoring Instrument. *Atmos. Meas. Techn.* **2011**, *4* (9), 1905–1928 DOI: 10.5194/amt-4-1905-2011.
- (57) Lee, C.; Martin, R. V.; van Donkelaar, A.; Lee, H.; Dickerson, R. R.; Hains, J. C.; Krotkov, N.; Richter, A.; Vinnikov, K.; Schwab, J. J. SO₂ emissions and lifetimes: estimates from inverse modeling using in situ and global, space-based (SCIAMACHY and OMI) observations. *J. Geophys. Res.: Atmos.* **2011**, *116*, D06304 DOI: 10.1029/2010JD014758.
- (58) Clarisse, L.; Clerbaux, C.; Dentener, F.; Hurtmans, D.; Coheur, P. Global ammonia distribution derived from infrared satellite observations. *Nat. Geosci.* **2009**, *2* (7), 479–483 DOI: 10.1038/ngeo551.